

## ON THE DEVELOPMENT OF MHD ASSISTED HYPERSONIC AIR INLETS

**Marco A. S. Minucci**

**Henry T. Nagamatsu**

**Leik N. Myrabo**

Rensselaer Polytechnic Institute

Troy, NY, USA

**Abstract** *Two MHD assisted hypersonic air inlets for advanced propulsion concepts are being currently tested in the Rensselaer Polytechnic Institute-RPI 65 cm Hypersonic Shock Tunnel. The first one, showing an axisymmetric geometry, fitted with 24 open-top MHD channels on its periphery and two pulsed Bitter type coils, was successfully tested at Mach 7,8. Appropriate reservoir temperature and pressure, 4.100 K and 850 psi, generated by the shock tunnel, provided the needed air electric conductivity behind the conical shock wave. The tests indicated that, due to the interaction of the high speed, high temperature, airflow in the channels and the perpendicular pulsed magnetic field, the hypersonic airflow, past the channels, was decelerated. Laser based Schlieren and luminosity photographs revealed the flow deceleration due to energy extraction. The extracted voltage was also recorded as a function of the electrical external resistor. Due to the model complexity and the lack of a second power supply, the acceleration of the conducting airflow past the MHD channels could not be attempted. To overcome this problem, a second inlet displaying a 2-D geometry, one open-top MHD Channel and permanent Nd-Fe-Bo magnets, is presently undergoing tests in the RPI facility.*

**Key Words:** *Magnetohydrodynamics, Hypersonics, Air inlets, Shock tunnel, Laser propulsion*

### 1. INTRODUCTION

In the 60's there was an active interest on the problem of the interaction of high velocity plasma with a magnetic field, (Rosa, 1962, Nagamatsu & Sheer, 1961, Nagamatsu *et al.*, 1962, Way *et al.*, 1961, Steg & Sutton, 1960). The need for better understanding of the MagnetoHydroDynamic, MHD, phenomena arose from the interest in thermonuclear reactions, astrophysics, electric power generation, space propulsion, and application of MHD for aerodynamic control of ICBM nose cones ( Ericson *et al.*, 1962) and the Apollo vehicle. Until today, numerous analytical and only limited experimental papers were published on the hypersonic MHD phenomena.

In the present, interest in MHD for aerospace applications has regrown spurred by the need to drastically decrease the cost of launching transatmospheric vehicles (Covault, 1999, Gurijanov *et al.*, 1996). A laser or microwave beamed energy with a MHD fanjet to accelerate the vehicles to orbital Mach number of 25 has been proposed by Myrabo *et al.* (1995). The inlet of this hypersonic engine is a novel device that enable active control of a Lightcraft, which is a vehicle that derives its power for flight propulsion from a beam of electromagnetic energy (laser or microwaves), Fig. 1. For the lift-off of the Lightcraft, Myrabo *et al.* (1995, 1998) and Mead *et al.* (1998) suggested the concept of Pulsed Detonation Engine (PDE) cycle. In this cycle, the engine develops laser-generated

thrust upon the aftbody of the Lightcraft. Laser energy is focused by the parabolic shaped aftbody mirror towards the center of the cowl surrounding the body and detonation waves are produced, Fig. 1. Recent flight tests, Fig. 2, conducted at High Energy Laser System Test Facility (HELSTF), White Sands Missile Range, New Mexico, successfully demonstrated the PDE cycle (Myrabo *et al.*, 1998, Mead *et al.*, 1998). These tests employed the output beam of a pulsed (10 Hz), high energy (1 kJ per pulse) carbon dioxide laser. The interest in developing a MHD assisted hypersonic air inlet for the Lightcraft concept motivated the present investigation.

## **2. EXPERIMENTAL APPARATUS**

### **2.1 Shock tunnel and related instrumentation**

A detailed description of the Rensselaer Polytechnic Institute-RPI 65 cm hypersonic shock tunnel can be found elsewhere (Minucci, 1991, Minucci *et al.*, 1994). For the present investigation, the tunnel was operated in the equilibrium interface mode (Minucci *et al.*, 1994) using Argon as the gaseous piston (Nascimento *et al.*, 1997,1998), near ambient temperature Helium as the driver gas and air as the test gas. In this mode of operation, the RPI facility can generate high enthalpy reservoir conditions, 4.100 K, temperature, 850 psi, pressure, upstream of the nozzle entrance for approximately 4 ms. By conveniently selecting the throat diameter, a free stream Mach 7,8 airflow is produced in the test section. The combination of the high enthalpy reservoir conditions and free stream Mach number, in turn, assure the minimum necessary electrical conductivity of the air flowing behind the conical shock wave standing around the model during the short (4 ms) useful test time. A Maxwell capacitor bank provides the high current-high voltage pulse, which drives the two Bitter type coils installed inside the model. The capacitor bank and the coils were donated by the US Army to the RPI Hypersonic Laboratory. The capacitor bank is connected to the shock tunnel test section via a copper coaxial power line. An in-house designed and built ceramic feed-through plate enables the power line to go through the test section steel wall, connecting the capacitor bank to the model. In the axisymmetric model tests, the coaxial line, inside the test section, is hooked up to the two Bitter coils, while in the 2-D model (wedge), it is connected to the two copper electrodes. An electronic controller, developed in-house by a graduate student, fires the capacitor bank shortly after the flow is established in the test section. The same controller also pulses the 15 W Oxford Lasers copper vapor laser and operates the camera mechanical shutter so that a Schlieren photograph can be taken. The photograph is synchronized with the magnetic/electric pulse generated by the discharge of the capacitor bank. The laser and the camera are part of a single pass Schlieren system designed for flow visualization inside the test section through the two 229mm diameter circular windows. Pressure data, measured by PCB pressure transducers installed in the model and in the tunnel, as well as shock tunnel heat transfer gages, voltage data from the model, and the electric current reading from the capacitor bank discharge are recorded by a Tektronix VXI and Test Lab data acquisition systems. These systems are integrated through the use of a computer code written by a graduate student using Labview™ software. Figure 3 shows a schematic view of the end of the hypersonic shock tunnel driven section indicating the apparatus described above.

### **2.2 Axisymmetric hypersonic inlet model**

The model consists of a Plexiglas™ outer shell fore body that houses two identical Bitter type coils mounted in an opposing, buckle, configuration in order to provide a stronger magnetic field on its periphery. This 178mm diameter shell replicates the Lightcraft vehicle fore body and it is fitted with 24 electrode fins. The electrode fins are made from circuit board material, 3.2mm thick, which consists of two outer thin copper layers separated by a fiberglass core. The 24 electrode fins were initially connected to each other in parallel. However, due to experimental difficulties, only two of

them were active and generated the data discussed in the present paper. The outer shell and the two magnets were kept in place by means of a center stainless steel hollow shaft fitted with two strong nuts designed to overcome the magnetic repulsive force between the coils during the run. Magnetic fields as high as 13 Tesla were produced at the coils center line and up to .2 Tesla at the model periphery. Initially, the coils were separated by an iron core made of laminated metal. The objective was to strengthen the magnetic field but due to electric arcing and very little change in the field, a Lucite™ disk was used instead. The stainless steel shaft was also used to attach the model to the shock tunnel test section main sting support system. Three impact pressure probes, 120 degree apart, were used to measure the Pitot pressure downstream of three selected open-top MHD channels. The objective of these probes was to record any dynamic pressure change due to the flow deceleration in the channels due to the energy extraction process. In the final configuration, different electric resistors were soldered across one of the 24 MHD channels to dissipate the electric power generated by the interaction of the high speed air plasma with the normal pulsed magnetic field. An additional impact pressure probe, installed off-center, registered the free stream Pitot pressure, enabling, in conjunction with shock the tunnel reservoir pressure and temperature measurements, the determination of the free stream conditions. These conditions were calculated by using the aforementioned measurements and computer codes modeling the shock tunnel flow and the equilibrium isentropic expansion in the nozzle developed by Minucci, 1991. Two thick copper cables connected the magnetic coils to the coaxial power line end inside the test section. The coupling between the coils and the cables as well as between the cables and the coaxial line had to be made very strong to support the repulsive forces during the capacitor bank discharge, so that electric arcing could be prevented. Figure 4 portrays an actual view of the axisymmetric inlet model installed in the tunnel test section.

### **2.3 2-D hypersonic inlet model**

Due to the inherent complexities found in the axisymmetric inlet model, such as large number of MHD channels, complex inlet flow, low degree of ionization provided by the conical shock wave, low magnetic field and lack of an additional power supply to try to accelerate the hypersonic air flow, a new inlet model was designed and constructed. This new inlet exhibits a much simpler design enabling a rapid evaluation of the MHD channel inlet flow conditions. It can be regarded as the 2-D version of one of the 24 channels existing in the axisymmetric inlet model. Also, by using permanent strong, 1,2 Tesla, magnets, no power supply is necessary during the energy extraction experiments. Each one of the Neodymium-Iron-Boron magnets measures 50,8mm X 38.1mm X 12,7mm and are commercially available from Edmund Scientific. Two of such magnets were glued together to create the bottom of the MHD channel measuring 50.8mm wide by 76.2mm long. They were then mounted to a cold rolled steel back plate 6,4mm thick and epoxied into a pocket, machined in the wedge top surface, in between the two electrodes. Since no power is required to drive these magnets, during flow acceleration attempts, the already existing capacitor bank will be available to power the two solid copper electrodes. Since the new 2-D model consists basically of a 254mm wide wedge with a 40 degree flow deflection angle, the Mach 7.8 oblique shock wave will produce a higher degree of ionization than the oblique shock in the axisymmetric model case. Also, because the model is symmetric with respect nozzle exit horizontal plane (the total wedge included angle is 80 degree) and the permanent magnet, along with the two electrodes, are installed only in the top surface, in one experiment it will be possible to observe both the MHD disturbed (top) and undisturbed (bottom) wedge flows. The wedge material is Delrin™ and, due to its relative softness, the model is fitted with a removable Delrin™ leading edge, so that it can be replaced due to the wear caused by the particles contaminating the hypersonic airflow exiting the nozzle. The inlet is instrumented with two surface pressure taps and two impact pressure probes. One of the surface pressure taps is located in the model centerline immediately downstream of the MHD channel exit, in the wedge upper surface.

The second one is located in the bottom wedge surface centerline, at the same distance from the model leading edge as the first one. The two impact pressure probes can be adjusted vertically so that the dynamic pressure distribution downstream the MHD channel centerline can be determined. The impact pressure probes are mounted symmetrically with respect to the nozzle exit horizontal plane so that both dynamic pressures, downstream the MHD channel (top wedge surface) and downstream the oblique shock wave (bottom surface) can be measured simultaneously. A third impact pressure probe, located outside the model, measures the free stream pitot pressure necessary to determine the nozzle exit flow conditions. As in the axisymmetric inlet model, PCB model M112A22 piezoelectric pressure transducers were used in all model probes and surface pressure taps. A hollow stainless steel shaft connects the model to the test section main sting support system and conveys the pressure transducer cables to a vacuum feed through. For the energy extraction experiments, different electric resistors are connected across the two electrodes, via copper bus bars. The voltage across the resistor is also monitored, and electric leads from the resistor terminals are housed by the hollow shaft and directed to the vacuum feed through.

The rectangular, 19,1mm X 76,2mm, electrodes, 54mm apart, are removable, so that different electrode shapes and concepts can be tested. In order to minimize flow disturbances, the electrodes have sharp leading edges and the ramp surfaces face outside the channel. Two tiny, 1mm diameter, holes near the electrode leading edges enable the use of a copper fuse wire to start the discharge during the flow acceleration attempts. Solid treaded copper rods, under the wedge top surface, connect the electrodes to the cables that bring the power from the capacitor bank.

At the time the present paper was written, the 2-D inlet model tests were being initiated. As a consequence, only the axisymmetric hypersonic inlet results will be discussed in the following section. An actual photograph of the 2-D model before its installation in the hypersonic shock tunnel test section is shown in Fig. 5.

### **3. PRELIMINARY EXPERIMENTAL RESULTS**

#### **3.1 Free stream conditions**

Figures 6 and 7 show typical reservoir and impact pressure traces, respectively, obtained during a shock tunnel run when the Bitter coils were pulsed. From these figures one can easily see that the capacitor bank discharge greatly affects the traces by clipping them. Since the reservoir pressure transducer is located just upstream of the nozzle entrance, outside the test section, and the impact pressure probe is installed near the nozzle exit, inside the test section, the electromagnetic noise generated by the capacitor discharge affects both locations. In spite of that, it is also possible to observe that, immediately before the discharge, the traces are reasonably flat, indication of fully developed flow conditions. These flow conditions correspond to a free stream Mach number 8 and reservoir pressure and temperature of 850 psi and 4.100 K, respectively.

#### **3.2 Natural luminosity photographs**

Figure 8 shows open shutter photographs of the luminous hypersonic airflow past the inlet with, right photograph, and without the magnetic field, left photograph. The large flow spillage seen in Fig. 8, photograph to the right, indicates that when the coils are pulsed, and electric energy is extracted through the electrodes, the airflow is substantially decelerated. For these particular photographs, all the 24 MHD channels were connected in parallel to an electric resistor that dissipated the power generated by the flow deceleration.

#### **3.3 Schlieren photographs**

Figure 9 shows Schlieren photographs of the hypersonic flow entering one of the 24 MHD channels with and without the magnetic field pulse, using the apparatus described previously. The

photograph to the right was taken simultaneously with the application of the magnetic field normal to the flow direction. By comparing the position of the conical shock wave, near the leading edge of the electrode in this photograph, with the position of the shock in the photograph to the left, one can easily see that, when the magnetic field is applied, the shock wave moves forward, into the flow. This is a clear indication that the inlet flow is being decelerated as a consequence of the magnetic field and the energy extraction.

### **3.4 Pitot pressure measurements**

As described previously, three Pitot pressure probes located downstream of three MHD channels 120 degree apart were used to quantify the flow deceleration. However, during the coils pulse, the electromagnetic noise clipped the output traces of the pressure transducers precluding any conclusive measurement. Nevertheless, it is of interest to point out that immediately before and after the magnetic pulse the output of the pressure transducers was normal. This behavior is believed to have been caused by the fact that the transducers have built in amplifiers, which are susceptible to strong electromagnetic interference. Another possible cause could have been the type of output cables used with the pressure transducers, which were not shielded.

### **3.5 Electric power extraction experiments**

Due to variations in the air plasma conductivity in each one of the 24 MHD channels, reliable data could only be obtained when power was extracted from an isolated pair of electrodes. This was accomplished by physically disconnecting a particular pair of electrodes, as shown in Fig. 9, from the rest of them and by measuring the voltage across an electric resistor connected in series with the selected electrode fins. From the recorded output voltage,  $U$ , trace and the known resistance,  $R$ , of the electric resistor, the electric current,  $I$ , can be determined as being  $I = U/R$ . Conversely, the electric power,  $P$ , being dissipated in the resistor is found to be  $P = U.I$ .

A typical voltage output trace from the selected pair of electrodes is shown in Fig. 10. Data was reduced using the two voltage peaks seen in Fig. 10 and the output voltage  $X$  electric current plot is shown in Fig. 11 for low external resistances. A possible explanation for the scattering observed in Fig. 11 is the very low electric conductivity of the airflow behind the conical shock wave entering the MHD channel. The low electric conductivity associated with a low transverse magnetic field,  $\sim .2$  Tesla, may have precluded a strong MHD interaction contributing to the erratic behavior observed in Fig. 11. Another possible reason could have been the effect of boundary layers over the electrode fins decreasing even more the net air electric conductivity in the MHD channel.

Figure 12 shows the variation of the extracted power with the electric current. For an ideal generator, this curve should have the shape of a parabola and this may indicate that, for the reasons stated above, MHD effects are still weak. Nevertheless, since Fig. 12 shows an increase of power with the increasing current, i.e., decreasing of external resistance, it may also indicate that the present tests were conducted near the beginning of the power curve.

## **5. CONCLUSIONS AND FURTHER RESEARCH**

Two MHD assisted hypersonic inlets have being designed and built for testing in the RPI .6m diameter hypersonic shock tunnel. At the time of preparation of the present manuscript, only preliminary experimental data was obtained for the axisymmetric inlet at a free stream Mach of 7,8 and reservoir pressure and temperature of 850 psi and 4.100 K, respectively. These data, which included luminosity and Schlieren photographs as well as electric energy extraction from the hypersonic flow, indicated that the airflow past the inlet can indeed be changed by MHD effects. More specifically, the results indicated that the hypersonic air stream around the inlet can be

decelerated and electric power can be generated at the cost of such deceleration and interaction with a magnetic field. However, due to the low values of air electric conductivity and transverse magnetic field, the power extraction data show some scattering. The hypersonic boundary layer over the electrode fins may also have played an important role in decreasing the net air conductivity in the MHD channel, further departing the results from an ideal electric generator behavior.

Testing of the 2-D MHD assisted hypersonic inlet is scheduled to begin shortly as the model has been already installed in the test section of the hypersonic shock tunnel. This model is fitted with stronger permanent magnets, surface pressure and Pitot pressure probes. In addition to the stronger magnetic field, due to the fact that the oblique shock wave produced by the wedge flow deflection angle of 40 degree is stronger than the conical shock wave produced by the axisymmetric inlet, the air conductivity behind the latter shock wave will be inherently higher. These improvements over the axisymmetric model are expected to produce more consistent voltage and power extraction data. Also, because the 2-D inlet will not need the capacitor bank to power the magnet, it will be used to drive current across the electrodes in an attempt to accelerate the electrically conductive airflow.

### ***Acknowledgments***

This report was prepared under Grant No. NAG8-1290 from NASA Marshall Space Flight Center. The authors would like to express their gratitude to Ms. Joyel M. Kerl and Messrs. Dean Meloney and Donald G. Messitt for their help in conducting the tests in the hypersonic shock tunnel. Also, the second author would like to acknowledge the support for his Post-Doctoral Program at the Rensselaer Polytechnic Institute from the Brazilian Air Force.

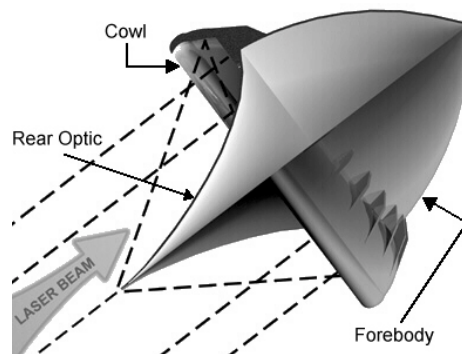


Figure 1-The Lightcraft transatmospheric vehicle concept.



Figure 2 –Lightcraft model in vertical flight in White Sands Missile Range, New Mexico.

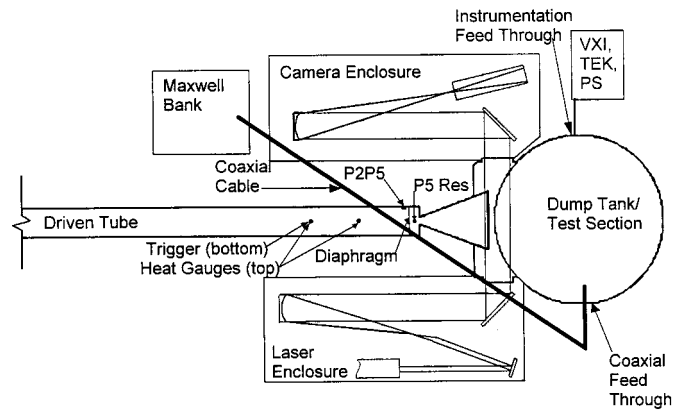


Figure 3-Layout of the instrumentation by the hypersonic shock tunnel test section.

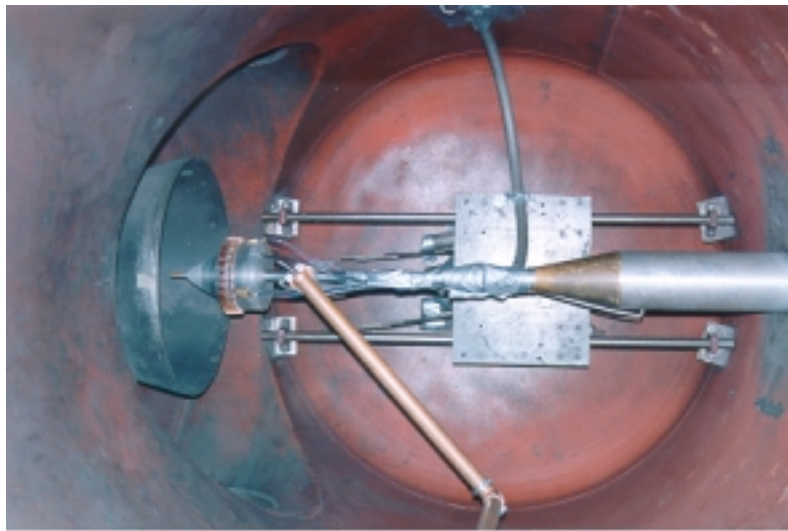


Figure 4-View of the MHD assisted axisymmetric hypersonic air inlet in the tunnel test section.

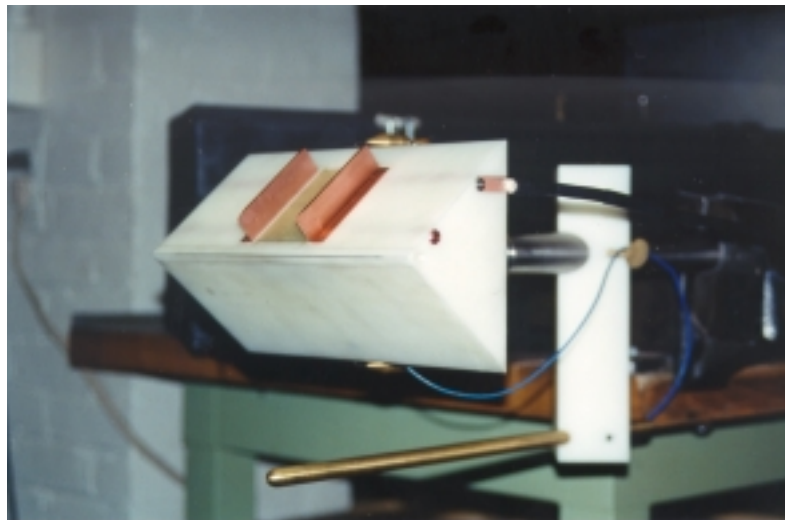


Figure 5- Photograph of the MHD assisted 2-D hypersonic air inlet prior to installation in the tunnel test section.

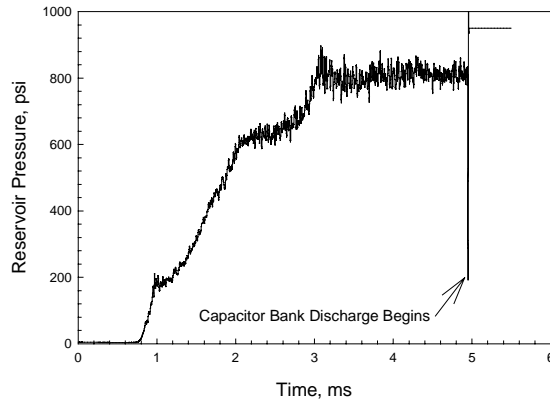


Figure 6-Typical reservoir pressure trace obtained during the capacitor bank discharge.

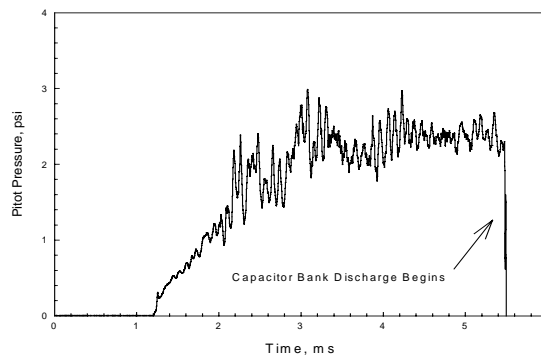


Figure 7- Typical main impact pressure trace obtained during the capacitor bank discharge.



Figure 8- Open shutter photographs of the luminous Mach 7,8 airflow past the inlet with the magnetic field off, left, and on, right. Flow is from left to right.

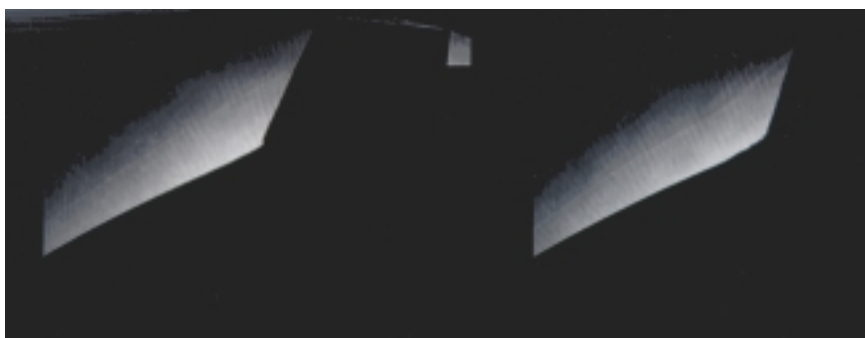


Figure 9-Schlieren photographs of the Mach 7,8 airflow near the electrode fins with the magnetic field off, left, and on, right. Flow is from left to right.

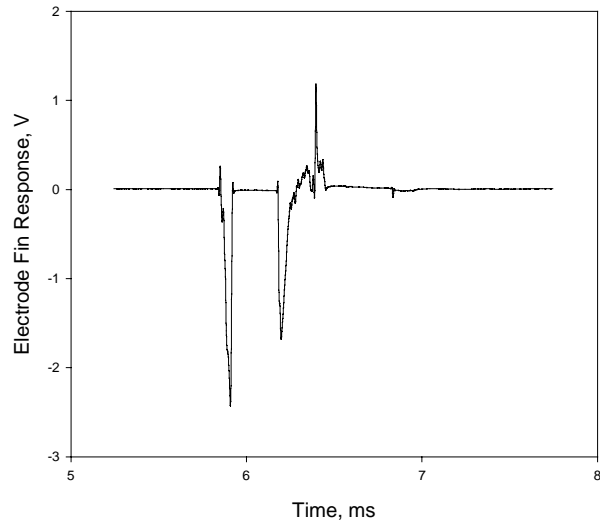


Figure 10- Typical voltage output trace from the selected pair of electrode fins.

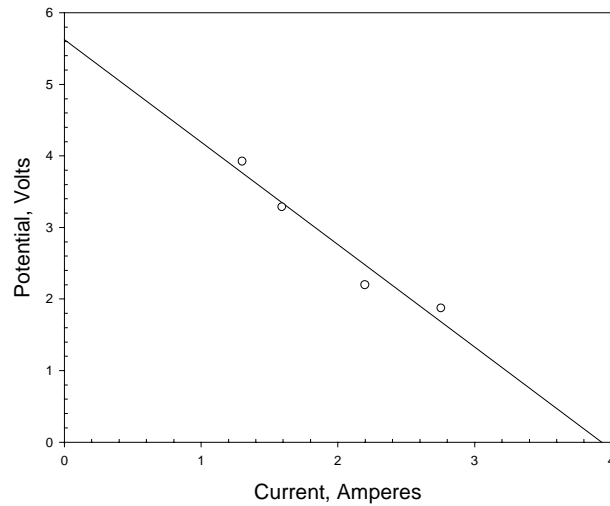


Figure 11- Output voltage as a function of the extracted electric current for low external resistance.

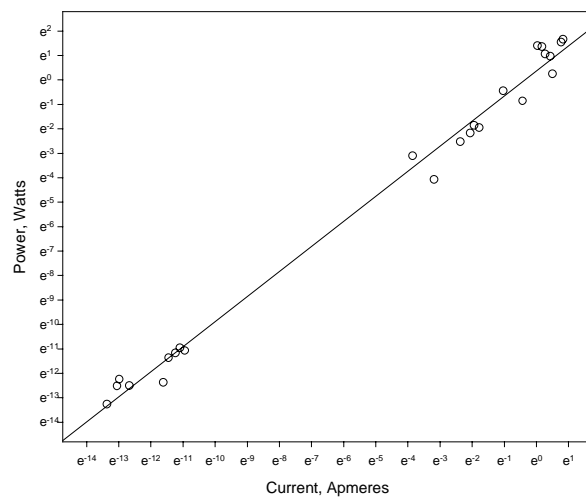


Figure 12- Extracted electric power as a function of the electric current.

## REFERENCES

- Covault, G. " 'Global Presence' Objective Drives Hypersonic Research," *Aviation Week & Space Technology*, April 5, 1999, pp. 54-58.
- Ericson, W.B., Maciulaitis, A., Spagnolo, F.A., Loeffler, A.L. Jr., Scheuing, R.A., and Hopkins, H.B. Jr., "An Investigation of MHD Flight Control," Grumman Aircraft Engineering Corp., National Electronics Conference, Dayton, Ohio, May, 14-16, 1962.
- Gurijanov, E.P., Harsha, P.T. " AJAX: New Directions in Hypersonic Technology," AIAA Paper 96-4609, 1996.
- Mead, F.B. Jr., Myrabo, L.N., and Messitt, D.G., "Flight and Ground Tests of a Laser-Boosted Vehicle," AIAA Paper 98-3735, July 1998.
- Minucci, M.A.S., "An Experimental Investigation of a 2-D Scramjet Inlet at Flow Mach Numbers of 8 to 25 and Stagnation Temperatures of 800 to 4.100 K," Ph. D. Thesis Dissertation, Department of Mechanical Engineering, Aeronautical Engineering & Mechanics, Rensselaer Polytechnic Institute, Troy, New York, USA. May 1991.
- Minucci, M.A.S., Nagamatsu, H.T. , "Hypersonic Shock-Tunnel Testing at an Equilibrium Interface Condition of 4100 K," *Journal of Thermophysics and Heat Transfer*, Vol. 7, No. 2, 1994, pp. 251-260.
- Myrabo, L.N., Mead, D.R., Raizer, Y.P., Surzhikov, and Rosa, R.J., "Hypersonic MHD Propulsion System Integration for a Manned Laser-Boosted Transatmospheric Aerospacecraft," AIAA Paper, June 1995.
- Myrabo, L.N., Messitt, D.G., and Mead, F.B. Jr., "Ground and Flight Tests of a Laser Propelled Vehicle," AIAA Paper 98-1001, January 1998.
- Nagamatsu, H.T., and Sheer, R.E.Jr., "Magnetohydrodynamics Results for Highly Dissociated and Ionized Air Plasma," *The Physics of Fluids*, Vol. 9, September 1961, pp.1073-1084.
- Nagamatsu, H.T., Sheer, R.E. Jr., and Weil, J.A., "Non-Linear Electrical Conductivity of Plasma for Magnetohydrodynamic Power Generation," ARS Paper 2632-62, November 1962.
- Nascimento, M.A.C., "Gaseous Piston Effect in Shock Tube/Tunnel When Operating in the Equilibrium Interface Condition," Ph.D. Thesis Dissertation, Instituto Tecnológico de Aeronautica – ITA, Sao Jose dos campos, Sao Paulo, Brazil, October 1998.
- Nascimento, M.A.C., Minucci, M.A.S., Ramos, A.G., and Nagamatsu, H.T., "Numerical and Experimental Studies on the Hypersonic Gaseous Piston Shock Tunnel," *Proceedings of the 21<sup>st</sup> International Symposium on Shock Waves*, September 1997.
- Rosa, R.J., "Magnetohydrodynamic Generators and Nuclear Propulsion," *ARS Journal*, August, 1962, pp.1221-1230.
- Steg, L. and Sutton, G.W., "The Prospects of MHD Power Generation," *Astronautics* 5, August 1960, pp.22-25.
- Way, S., DeCorso, S.M., Hundstud, R.L., Kenney, G.A., Stewart, W., and Young, W.E., "Experiments with MHD Power Generation," *Trans. Am. Soc. Mech. Eng., J. Eng. Power* 83, Series A. October 1961, pp.394-408.